ACS chemical biology

Letters

pubs.acs.org/acschemicalbiology

Genetically Encoded Photo-cross-linkers Map the Binding Site of an Allosteric Drug on a G Protein-Coupled Receptor

Amy Grunbeck,[†] Thomas Huber,[†] Ravinder Abrol,[‡] Bartosz Trzaskowski,[‡] William A. Goddard, III,[‡] and Thomas P. Sakmar*,[†]

[†]Laboratory of Molecular Biology & Biochemistry, The Rockefeller University, 1230 York Ave., New York, New York 10065, United States

[‡]Materials and Process Simulation Center (MC 139-74), California Institute of Technology, 1200 E. California Blvd., Pasadena, California 91125, United States

Supporting Information

ABSTRACT: G protein-coupled receptors (GPCRs) are dynamic membrane proteins that bind extracellular molecules to transduce signals. Although GPCRs represent the largest class of therapeutic targets, only a small percentage of their ligand-binding sites are precisely defined. Here we describe the novel application of targeted photo-cross-linking using unnatural amino acids to obtain structural information about the allosteric binding site of a small molecule drug, the CCR5-targeted HIV-1 co-receptor blocker maraviroc.

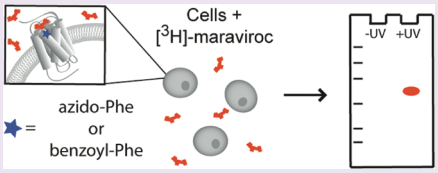

Many G protein-coupled receptor (GPCR)-modulated signaling pathways are involved in human disease, and GPCRs are a major target class for small molecule therapeutics and biologicals.[1] Some GPCR-targeted drugs bind to orthosteric sites and inhibit the binding interactions with endogenous agonist ligands that are necessary to form productive signaling complexes. However, GPCR-mediated signaling can also be affected by allosteric modulators.[2,3] Targeting potential allosteric sites on GPCRs opens up new avenues for structure-based drug design.[1] To facilitate future drug development and to understand the mechanism of action of existing drugs, it is important to identify the binding sites of both orthosteric and allosteric GPCR modulators.[4,5] However, it is not straightforward to identify the precise binding sites and mechanisms of action of GPCR ligands. For example, it is known that GPCRs bound to antagonists or agonists display different packing within the 7-helix bundles, and it is likely that receptor activation proceeds through a series of agonist-GPCR conformations. In addition, computational predictions suggest that binding of various antagonists to CCR5 stabilizes different packings within the 7-helix bundle, which might lead to changes in function (*e.g.*, coupling to β-arrestin or G protein). Here, we demonstrate the application of a chemically precise technique in live cells to define the binding site of a small molecule drug to an important GPCR drug target, and we reconcile the results with computational predictions.

Maraviroc, a small molecule HIV-1 entry inhibitor, is a GPCR allosteric modulator with inverse agonist activity (Figure 1a).[6] CC chemokine receptor 5 (CCR5), the molecular target for maraviroc,[7] is the primary co-receptor required for HIV-1 cellular entry.[8,9] Maraviroc is the first GPCR-specific HIV-1 entry inhibitor to be approved by the FDA for therapeutic use, but its precise receptor−drug binding site interactions have not been defined, and the mechanism for how the drug blocks HIV-1 entry remains controversial. The clinical relevance of co-receptor blocker agents and the increasing frequency of maraviroc-resistant viruses also signify the importance of investigating the binding interactions between CCR5 and maraviroc.[10] Understanding the precise binding orientation of maraviroc could contribute to the design of additional HIV-1 co-receptor blockers. In addition, recent advances in structural studies have confirmed that the arrangement and disposition of the 7-helix bundle of family A GPCRs is conserved. Since maraviroc is hypothesized to bind within a pocket in the 7-transmembrane helical domain of CCR5, determining the allosteric binding site for maraviroc could facilitate the design of other GPCR allosteric regulators.

A high-resolution crystal structure of a GPCR−ligand complex provides precise information about receptor−ligand contacts and binding interactions. In the absence of relevant crystal structures, other methods such as site-directed mutagenesis, competition-binding experiments that apply chemically modified ligands or analogues and chemical cross-linking experiments have been employed. In general, these methods share the inherent limitation that either the ligand under study or its target receptor needs to be significantly modified. Currently, there is no high-resolution structure of CCR5, and despite significant effort, including extensive receptor mutagenesis and medicinal chemistry that has created hundreds of small molecule CCR5 ligands, the precise binding site of maraviroc is not known experimentally. In order to identify amino acid residues in CCR5 that are close to bound maraviroc, we have applied an alternative targeted photo-

Received: February 8, 2012
Accepted: March 28, 2012
Published: March 28, 2012

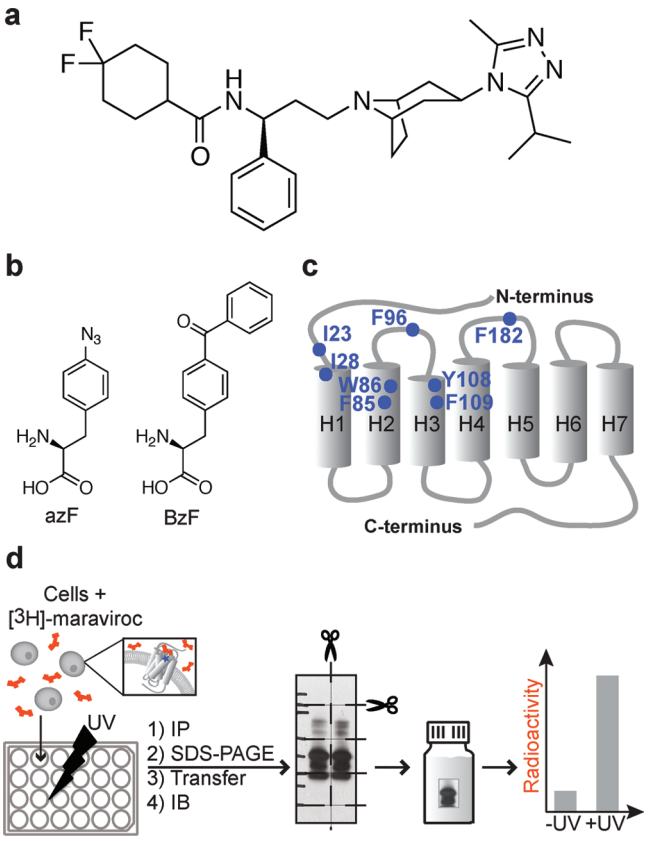

Figure 1. Targeted photo-cross-linking was employed to study the binding site of maraviroc on CCR5. (a) Chemical structure of the CCR5-specific HIV-1 entry inhibitor maraviroc. (b) The two UAAs containing photoactivable cross-linkers that were genetically incorporated into CCR5 in HEK293T cells using amber stop codon suppression. (c) Schematic of the CCR5 structure showing in blue the positions in the receptor where BzF and azF were introduced. (d) Experimental scheme for the targeted photo-cross-linking technology. The first step involves incubating HEK293T cells expressing the CCR5 UAA mutants with [^{3}H]-maraviroc. After incubation the cells were exposed to 365-nm UV light in a 24-well plate format. The cells were then lysed in detergent buffer solution, and receptors were immunopurified, run on an SDS-PAGE gel, transferred to a PVDF membrane, and immunoblotted to determine receptor expression. The sample lanes were then cut from the PVDF membrane, and each sample lane was cut into three different molecular weight segments. These membrane segments were then put into scintillation vials with scintillation fluid and then counted on a beta-scintillation counter to quantify the amount of radioactivity in each segment.

cross-linking technique that probes the binding of [^{3}H]-labeled maraviroc to a minimally altered receptor.

The targeted photo-cross-linking technology we used to investigate the maraviroc binding site is an adaptation of a method we previously developed to identify residues in CXC chemokine receptor 4 (CXCR4) that were within about 3 Å of a fluorescently labeled analogue of its peptide ligand, T140. The results from this experiment were benchmarked using the crystal structure of CXCR4 bound to a peptide ligand, CVX15, homologous to T140.[11,12] The obvious limitation of this earlier work was that in essence we mapped the binding site of a fluorescein-labeled analogue of T140 and not T140 itself. In the current work, we aimed to devise a strategy to study maraviroc binding without altering the structure of maraviroc. We therefore optimized the targeted photo-cross-linking technology in a small-scale cell-based system so that radioactivity could be used to detect the presence of maraviroc. This allowed us to use a tritiated version of maraviroc, which retained its native chemical structure and its pharmacological properties.

We have adapted the amber codon suppression technology to genetically incorporate photo-cross-linker unnatural amino acids (UAAs) into a GPCR.[13] The targeted photo-cross-linking technology allows for minimal perturbation to the protein structure by introducing the photoactivable cross-linkers as UAA side chains. We employed *p*-benzoyl-L-phenylalanine (BzF)[14] and *p*-azido-L-phenylalanine (azF),[15,16] which contain side chains of different sizes with unique photochemistries (Figure 1b).[17,18] BzF and azF were applied in parallel experiments at multiple sites in the receptor. The smaller size of the azF side chain compared with the BzF side chain allows for the investigation of positions in the receptor that are otherwise more sensitive to structural perturbations. In addition, the unique reactivity of each of these photo-cross-linking groups allows for the sampling, in principle, of different potential cross-links. Our previous work suggested that the carbonyl in the benzophenone moiety of BzF needs to be within 3 Å from its binding partner in order to form a covalent complex after photoactivation.[12] This distance constraint is also consistent with earlier studies using benzophenone-based cross-linkers.[17] The nature of the photoreactive species formed from phenylazide is controversial, but we make the assumption that the distance dependence of the cross-linking reaction is roughly the same as the benzophenone because we obtained similar cross-linking profiles with both BzF and azF in an earlier study.[12]

Several earlier studies proposed models of the maraviroc binding site in CCR5 based on scanning mutagenesis, molecular dynamics simulations, or structure−activity relationship studies.[19−21] Some of this work was based on studies of other structurally related CCR5 pharmacophores such as TAK-779.[22,23] From these earlier data, we chose 8 positions in CCR5 for additional study (Figure 1c). We chose these positions with the expectation, based on earlier mutagenesis data, that when mutated to either BzF or azF, a loss-of-function phenotype would not be observed. Our aim was to create a set of UAA mutant receptors that would bind maraviroc normally and in addition contain reactive side chains that might cross-link upon UV excitation.

We expressed each of the selected CCR5 mutants in HEK293T cells under conditions designed to incorporate either BzF or azF at the position of interest. Cells expressing the CCR5 UAA mutants were incubated with [^{3}H]-maraviroc and then exposed to UV light. Cells were lysed in detergent buffer solution, and receptors were immunopurified using 1D4 mAb. The immunopurified material was then run on an SDS-polyacrylamide gel to separate out any tritiated ligand that was not covalently bound to the receptor. After transferring proteins to a PVDF membrane and measuring receptor expression by immunoblot analysis, the PVDF membrane was then cut into strips to partition each sample. Each sample strip was cut further into segments, and the amount of radioactivity in each segment was measured (Figure 1d).

These experiments showed that 3 of the 8 positions in CCR5 engineered to contain either azF or BzF were able to cross-link to maraviroc upon UV illumination (Figure 2). Among the positions tested, different patterns of reactivity were noted for CCR5 containing azF *versus* BzF. Significant tritium was detected in the CCR5−maraviroc complex when either I28 or

dx.doi.org/10.1021/cb300059z | *ACS Chem. Biol.* 2012, 7, 967−972

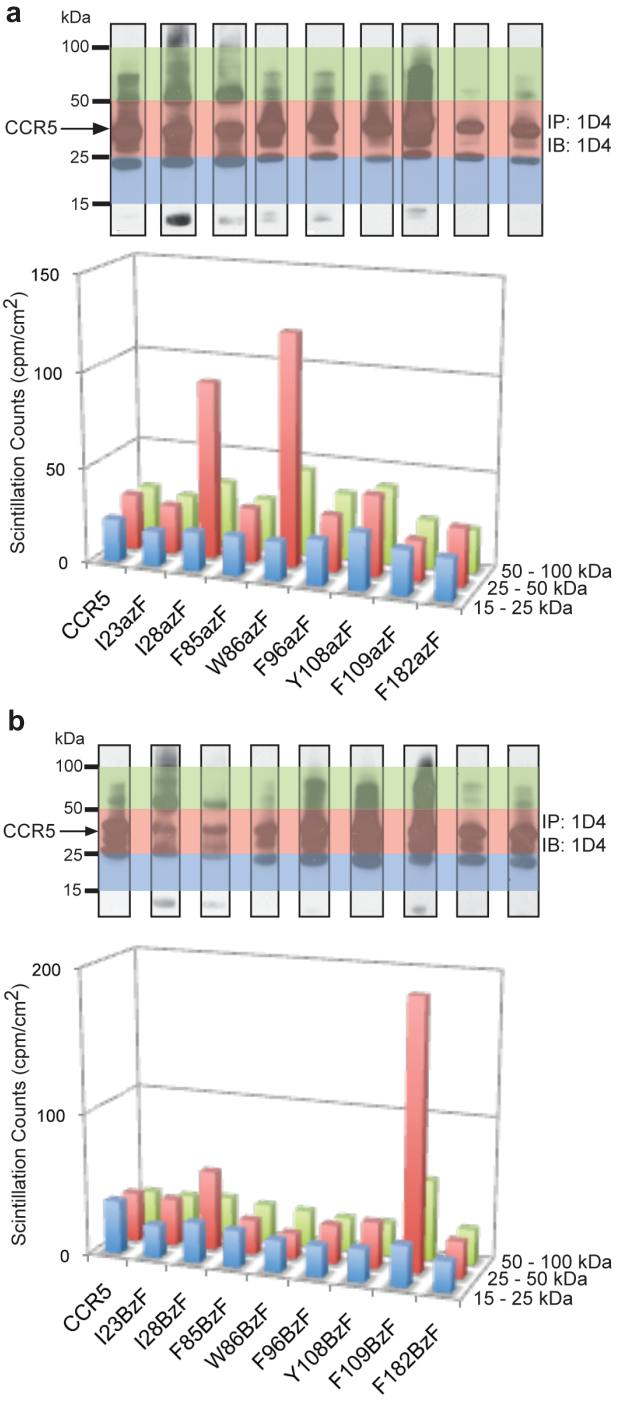

Figure 2. Photo-cross-linking results with CCR5 azF and BzF replacement mutants. (a) CCR5 azF mutants were tested for cross-linking to [^{3}H]-maraviroc. Receptor expression is shown by immunoblot analysis with the 1D4 antibody. Note that the exposure for each sample is not normalized across all lanes. Each lane corresponds to the mutant shown in the bar graph directly below. The colors highlighted on the Western blot designate where the membrane was cut for scintillation counting and correlate with the colors in the bar graph. The bar graph reports the amount of tritium detected in the PVDF segments indicated. All of these samples represent the CCR5 azF mutants that were exposed to UV light in the presence of [^{3}H]-maraviroc. The membrane segment of interest is the 25−50 kDa segment (red), which contains CCR5. The CCR5 band is indicated with the arrow at 37 kDa. The other strong band at 25 kDa is the light chain from the 1D4 mAb, which was used for immunopurification. Positions 28 and 86 were the only two sites found to have significantly higher tritium levels in the 25−50 kDa segment. (b) The same positions in CCR5 were also tested for cross-linking using BzF. This data set is displayed as in panel a. Positions 28 and 109 were found in this cross-linking scan to have significantly higher tritium levels in the 25−50 kDa segment.

W86 was replaced by azF. However, when BzF was incorporated at position I28, only a slight increase above background was detected. A significant increase in tritium levels was detected, however, when BzF was incorporated at position F109, a site that did not cross-link when azF was present.

For these 4 samples (I28azF-CCR5-maraviroc; W86azF-CCR5-maraviroc; I28BzF-CCR5-maraviroc; F109BzF-CCR5-maraviroc) the elevated levels of tritium were detected only in the 25−50 kDa gel fraction, which includes CCR5 with an apparent molecular mass of approximately 37 kDa. Since the molecular mass of maraviroc is under 500 Da, tritium only appears in the 25−50 kDa fraction if the [^{3}H]-maraviroc is covalently bound to CCR5. These cross-linking results were also found to be UV-treatment-specific (Supplementary Figures 1 and 2). From this information, we conclude that the elevated levels of tritium in the 25−50 kDa gel fractions are a result of a direct UV-dependent cross-link between the UAA incorporated into CCR5 and [^{3}H]-maraviroc. The cross-linking patterns observed with BzF and azF may differ as a result of either the structural orientation or reactivity of their unique side chains. Alternatively, the structural difference between the azido group and benzoyl group might have had differing effects on ligand affinity for the mutant CCR5.

We performed ligand-binding experiments with [^{3}H]-maraviroc to determine if introducing a UAA at any of the positions we tested altered maraviroc binding. Only the W86BzF-CCR5 mutant showed significantly decreased levels of binding to maraviroc (Supplementary Figure 3). This result suggests that W86BzF-CCR5 may have failed to cross-link to maraviroc because of decreased ligand binding affinity. On the other hand, we also detected different cross-linking results at position 109 for the two cross-linkers. The binding data suggest that maraviroc is able to bind to both the F109BzF-CCR5 and F109azF-CCR5 mutants. Therefore, we can conclude that the difference in cross-linking between the two photoactivable groups at position 109 was a result of a difference in reactivity of the photoactivatable cross-linking groups. Other relevant factors that might affect the reactivity of these cross-linking groups include the chemical bonds of maraviroc near to the reactive moiety and the specific spatial orientation of the side chain.

We further evaluated our cross-linking results using a newly predicted structure of the CCR5−maraviroc complex, which was obtained by using the GEnSeMBLE structure prediction methodology.[24] This methodology (summarized in the Supporting Information) is a Monte Carlo based method aimed at sampling all reasonable packings of the 7-helix bundle (we examined 10 trillion) and selecting an ensemble of 100 low-energy packings likely to play a role in binding of various ligands and in the activation process. The lowest 20 of these structures were used to predict the most stable CCR5−maraviroc complex, which was used to understand the experimental observations. We selected this predicted structure to calculate 100 different conformations of the BzF and azF side chains at each of the eight positions in CCR5 that were tested

dx.doi.org/10.1021/cb300059z | ACS Chem. Biol. 2012, 7, 967−972

in the cross-linking studies. Distance measurements were then made from either the carbonyl in BzF or the nitrogen adjacent to the phenyl ring in azF to the nearest possible non-hydrogen atom in maraviroc. We then calculated a probability distribution for the side chain at each of the indicated positions to come within 3 Å of contacting a non-hydrogen atom in maraviroc (Figure 3). According to the predicted structures, the only positions in CCR5 with a reasonable probability of being within 3 Å of the bound maraviroc were W86, Y108, and F109.

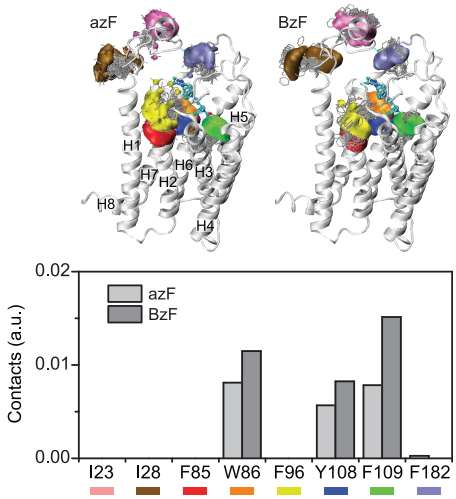

Figure 3. Interpretation of cross-linking data according to a molecular model of the CCR5−maraviroc complex. The cross-linking experiments identified three positions in the receptor that were able to cross-link to maraviroc when replaced by either azF or BzF. These results suggest that these three positions in CCR5 are within ∼3 Å from the bound maraviroc. We modeled 100 different conformations of the azF and BzF side chains at each of the positions tested in the cross-linking experiments in the context of this CCR5−maraviroc model. We then measured the distance from the reactive group in the photo-cross-linker, which is the carbonyl in BzF or the nitrogen adjacent to the phenyl ring in azF, to the nearest non-hydrogen atom in maraviroc. The top panel in this figure displays the CCR5−maraviroc model with the side chain predictions at each of the positions in CCR5 that were replaced with a UAA. The colored densities represent the location of the reactive group in azF (left) and BzF (right), and the colors coordinate with the colored boxes under the residue names listed below the bar graph. The bar graph shows the probability of the side chains at the indicated position to be within 3 Å of contacting a non-hydrogen atom in maraviroc. In this model only W86, Y108, and F109 are found to be within 3 Å of the bound maraviroc. Experimentally, cross-linking was also found between I28BzF-CCR5 and maraviroc.

The experimental cross-linking data are consistent with the predictions based on the W86 and F109 positions in the CCR5−maraviroc complex. On the other hand, our predicted model suggested that Y108 would be within cross-linking distance of bound maraviroc, but no experimental cross-link was observed under the conditions tested. This discrepancy between predictions based on the complex model and the experimental data could mean that the complex model is not entirely correct (although the other sites were accurately predicted). One possible explanation is that CCR5 might adopt a different low-energy conformation for Y108BzF and Y108azF mutants. This is plausible because we found that the Y108A mutant does adopt a different transmembrane bundle packing when bound to maraviroc (data not shown). If the CCR5−maraviroc complex for the UAA-containing protein does not change, a second possibility for the discrepancy could be that the photo-cross-linkers at position 108 were not able to react due to *either* a suboptimal orientation of the side chain *or* the lack of an appropriate target bond in maraviroc. Both of these possible explanations are plausible because Y108 side chain lies in a tight region near maraviroc, whereas both W86 and F109 reside in a more open region. Thus, to accommodate the BzF and azF UAAs at the Y108 position, maraviroc may have to move to a different (but may be proximal to original) binding site not accessible to the photo-cross-linkers. Our computational methods can be used to test these suggestions, but we have not yet done so. In addition, position 28, which formed cross-links in both the I28azF-CCR5 and I28BzF-CCR5 mutants, was not identified in the model to be within cross-linking distance of maraviroc. This result again could indicate limitations of the model. However, given the location of I28 in the N-terminal tail of CCR5, we favor the possibility that the experimental cross-link could suggest an additional maraviroc-binding site, which has also been predicted before by others and us.[6,25] The location of I28, is consistent with a maraviroc "docking site" on the extracellular surface of CCR5 and might be relevant for understanding its mechanism of action with respect to its function as an HIV-1 entry blocker. To further evaluate the exact orientation of maraviroc in the CCR5 ligand-binding pocket, we are in the process of identifying the locations of the cross-links on the maraviroc molecule. In addition, we will examine the effect of UAAs on the structure of CCR5 conformations.

We report here, to our knowledge, the first demonstration of a direct chemical cross-link between a GPCR and its native small-molecule ligand. We show that the targeted photo-cross-linking technology using UAA mutagenesis can be applied to identify the binding site of a small molecule ligand and that tritium is a sensitive detection tag for small-scale cell-based assays. We used the cross-linking results to evaluate a model of the CCR5−maraviroc complex and confirmed that maraviroc binds within the transmembrane helix bundle. This method should prove to be valuable for obtaining structural information about the binding site of GPCR allosteric modulators. In principle, the method should be applicable to any receptor−ligand complex where the receptor can be heterologously expressed in mammalian cells in culture and isotopically labeled ligands are available.

METHODS

Materials. [^{3}H]-Maraviroc was a generous gift from Bill Goddard and PharmSelex. 1D4 monoclonal antibody was obtained from the National Cell Culture Center. The goat anti-mouse antibody conjugated to horseradish peroxidase was purchased from VWR (catalogue no. 95059-094).

Site-Directed Mutagenesis and Plasmid Construction. The suppressor tRNA and BzF and azF amino-acyl tRNA synthetase plasmids were constructed as previously described.[13,15] The human CCR5 gene was in a pcDNA3.1(+) plasmid and contained a C-terminal 1D4-epitope, TETSQVAPA. The amber stop codons were introduced into CCR5 using the Quikchange Lightning Site-Directed Mutagenesis kit (Stratagene).

Expression of CCR5 Unnatural Amino Acids Mutants in Mammalian Cells. CCR5 UAA containing mutants were expressed in HEK293T cells as previously described.[12,13] In brief, HEK293T cells were transfected with three cDNA simultaneously using the lipofectamine plus reagent (Invitrogen). These cDNA contained the genes for the suppressor tRNA, amino-acyl tRNA synthetase, and human CCR5 amber mutant. The ratio of DNA in micrograms was 1:0.1:1 CCR5 amber mutant/tRNA synthetase/suppressor tRNA. For transfection of

dx.doi.org/10.1021/cb300059z | *ACS Chem. Biol.* 2012, 7, 967−972

one 10 cm plate, 3.5 μg of the CCR5 amber mutant DNA was used. WT CCR5 was transfected using 0.14 μg per 10 cm^2 plate in order to obtain comparable expression levels to the CCR5 UAA mutants. Cells were then grown in media containing 10% FBS with 0.5 mM of UAA in Dulbecco's Modified Eagle's Medium (DMEM; 4.5 g/L glucose, 2 mM glutamine; Gibco). Cells were used for photo-cross-linking experiments 48 h post-transfection.

Photo-cross-linking of Cells Expressing CCR5 UAA Mutants to [^{3}H]-Maraviroc. Two days post-transfection HEK293T cells were suspended in Dulbecco's phosphate buffered saline (DPBS; Gibco). Cells were then spun down and resuspended in Hank's Buffered Salt Solution (HBSS; pH 7.5) containing 20 mM HEPES with 0.2% BSA and 100 nM [^{3}H]-maraviroc. Cell suspensions were then incubated for 2 h at 37 °C on a nutator. After the incubation cell suspensions were transferred to a 24 well plate and exposed to a Maxima ML-3500S UV-A light (Spectronics Corporation) in a 4 °C cold room on ice for 15 min. After UV light exposure cells were transferred to eppendorf tubes and pelleted, and supernatant was removed. Cell pellets were then stored at −20 °C until further analysis.

Western Blot Analysis. Cell pellets were solubilized in 1% (w/v) *n*-dodecyl β-D-maltoside in 20 mM Tris pH 7.5 containing protease inhibitors for 1 h at 4 °C on a nutator. After solubilization the lysate was then spun down at 20,000 × *g* for 5 min. The supernatant was then bound to sepharose beads conjugated to the 1D4 antibody overnight at 4 °C. The next day the beads were washed three times with the 1% *n*-dodecyl β-D-maltoside buffer. Samples were then eluted from the beads by shaking the beads for 1 h at 37 °C in 1% SDS. Fifteen microliters of the eluted sample was then mixed with 5 μL of 4X NuPAGE LDS sample buffer containing DTT and then run on an SDS-PAGE gel (NuPAGE Novex 4−12% Bis-Tris Gel). The remaining eluted sample was stored at −20 °C for further characterization. The SDS-PAGE gel was then transferred to a polyvinylidene difluoride (PVDF) membrane for immunoblotting. The PVDF membrane was blocked in 5% milk in 1X TBST for 1 h at RT on a shaker followed by incubation with the primary monoclonal 1D4 antibody at 1:5000 dilution in 5% milk in 1X TBST overnight at 4 °C. After three washes with 1X TBST, the PVDF membrane was then incubated with an anti-mouse antibody conjugated to horseradish peroxidase at 1:10,000 in 5% milk in 1X TBST. The membrane was then incubated in Supersignal West Pico Chemiluminescent Substrate (Thermo Scientific) prior to being exposed to HyBlot CL auto-radiography film (Denville Scientific Inc.).

Quantification of [^{3}H]-Maraviroc Bound and Cross-Linked to CCR5 Mutants. After the PVDF membrane was exposed to film, the membrane was then cut into segments to quantify the amount of tritium present. The membrane was cut between each lane to separate each sample; in addition each sample was cut into three different molecular weight segments as specified. Each of these membrane segments were then transferred to individual vials with scintillation fluid and counted on a LKB Wallac 1209 Rackbeta Liquid Scintillation Counter (Perkin-Elmer). To quantify the amount of [^{3}H]-maraviroc that was bound to each of the CCR5 UAA mutants, 15 μL of the original eluted sample from the 1D4 mAb sepharose beads was transferred directly into a vial with scintillation fluid. All of the scintillation vials were mixed thoroughly before being counted on the beta-scintillation counter. Each vial was counted over 10 min. After counting, the counts per minute (cpm) per cm^2 of PVDF membrane was then calculated for each membrane segment by dividing the cpm for a particular sample by the area of the membrane segment in cm^2. The amount of [^{3}H]-maraviroc each CCR5 UAA was able to bind was normalized to the other mutants by setting the WT sample as 100% and then calculating for the UAA mutants what percentage they were of WT.

Molecular Modeling of CCR5 UAA Mutants. The CCR5−maraviroc complex model obtained as described above was used to predict 100 conformations of the azF and BzF side chains for each site examined in CCR5 using modeler.[26] These structures were analyzed for their potential to form a cross-link with maraviroc by determining the distance from the carbonyl in BzF or the nitrogen adjacent to the phenyl ring in azF to the nearest non-hydrogen atom in maraviroc. The contacts were calculated from the cumulative distribution function at a distance of 3 Å. The distance measurements and molecular graphics were made using VMD.[27]

■ ASSOCIATED CONTENT

Supporting Information

This material is available free of charge *via* the Internet at http://pubs.acs.org.

■ AUTHOR INFORMATION

Corresponding Author

*E-mail: sakmar@rockefeller.edu.

Notes

The authors declare no competing financial interest.

■ ACKNOWLEDGMENTS

We wish to thank M. Teintze and E. Dratz for helpful discussions and for providing reagents for use in ongoing work. We also thank M. Kazmi and K. Thapa for scientific assistance. W.A.G. acknowledges support in part through funding from PharmSelex and in part through gifts to the Materials and Process Simulation Center at Caltech. The Tri-Institutional Training Program in Chemical Biology supports A.G.

■ REFERENCES

(1) Salon, J. A., Lodowski, D. T., and Palczewski, K. (2011) Significance of G protein-coupled receptor crystallography for drug discovery. *Pharmacol. Rev. 63*, 901−937.

(2) Christopoulos, A., and Kenakin, T. (2002) G protein-coupled receptor allosterism and complexing. *Pharmacol. Rev. 54*, 323−374.

(3) Janz, J. M., Ren, Y., Looby, R., Kazmi, M. A., Sachdev, P., Grunbeck, A., Haggis, L., Chinnapen, D., Lin, A. Y., Seibert, C., McMurry, T., Carlson, K. E., Muir, T. W., Hunt, S., 3rd, and Sakmar, T. P. (2011) Direct interaction between an allosteric agonist pepducin and the chemokine receptor CXCR4. *J. Am. Chem. Soc. 133*, 15878−15881.

(4) Congreve, M., and Marshall, F. (2010) The impact of GPCR structures on pharmacology and structure-based drug design. *Br. J. Pharmacol. 159*, 986−996.

(5) Keov, P., Sexton, P. M., and Christopoulos, A. (2011) Allosteric modulation of G protein-coupled receptors: a pharmacological perspective. *Neuropharmacology 60*, 24−35.

(6) Garcia-Perez, J., Rueda, P., Staropoli, I., Kellenberger, E., Alcami, J., Arenzana-Seisdedos, F., and Lagane, B. (2011) New insights into the mechanisms whereby low molecular weight CCR5 ligands inhibit HIV-1 infection. *J. Biol. Chem. 286*, 4978−4990.

(7) Dorr, P. K., Todd, K., Irvine, R., Robas, N., Thomas, A., Fidock, M., Sultan, H., Mills, J., Perruccio, F., Burt, K., Rickett, G., Perkins, H., Griffin, P., Macartney, M., Hamilton, D., Westby, M., and Perros, M. (2005) Site-directed mutagenesis studies of CCR5 reveal differences in the interactions between the receptor and various CCR5 antagonists. *Abstr. Intersci. Conf. Antimicrob. Agents Chemother. 45*, 261.

(8) Deng, H., Liu, R., Ellmeier, W., Choe, S., Unutmaz, D., Burkhart, M., Di Marzio, P., Marmon, S., Sutton, R. E., Hill, C. M., Davis, C. B., Peiper, S. C., Schall, T. J., Littman, D. R., and Landau, N. R. (1996) Identification of a major co-receptor for primary isolates of HIV-1. *Nature 381*, 661−666.

(9) Dragic, T., Litwin, V., Allaway, G. P., Martin, S. R., Huang, Y. X., Nagashima, K. A., Cayanan, C., Maddon, P. J., Koup, R. A., Moore, J. P., and Paxton, W. A. (1996) HIV-1 entry into CD4(+) cells is mediated by the chemokine receptor CC-CKR-5. *Nature 381*, 667−673.

(10) Metz, M., Bourque, E., Labrecque, J., Danthi, S. J., Langille, J., Harwig, C., Yang, W., Darkes, M. C., Lau, G., Santucci, Z., Bridger, G. J., Schols, D., Fricker, S. P., and Skerlj, R. T. (2011) Prospective CCR5 small molecule antagonist compound design using a combined

mutagenesis/modeling approach. *J. Am. Chem. Soc. 133*, 16477−16485.
(11) Wu, B., Chien, E. Y., Mol, C. D., Fenalti, G., Liu, W., Katritch, V., Abagyan, R., Brooun, A., Wells, P., Bi, F. C., Hamel, D. J., Kuhn, P., Handel, T. M., Cherezov, V., and Stevens, R. C. (2010) Structures of the CXCR4 chemokine GPCR with small-molecule and cyclic peptide antagonists. *Science 330*, 1066−1071.
(12) Grunbeck, A., Huber, T., Sachdev, P., and Sakmar, T. P. (2011) Mapping the ligand-binding site on a G protein-coupled receptor (GPCR) using genetically encoded photocrosslinkers. *Biochemistry 50*, 3411−3413.
(13) Ye, S. X., Kohrer, C., Huber, T., Kazmi, M., Sachdev, P., Yan, E. C. Y., Bhagat, A., RajBhandary, U. L., and Sakmar, T. P. (2008) Site-specific incorporation of keto amino acids into functional G protein-coupled receptors using unnatural amino acid mutagenesis. *J. Biol. Chem. 283*, 1525−1533.
(14) Kauer, J. C., Erickson-Viitanen, S., Wolfe, H. R., Jr., and DeGrado, W. F. (1986) p-Benzoyl-L-phenylalanine, a new photoreactive amino acid. Photolabeling of calmodulin with a synthetic calmodulin-binding peptide. *J. Biol. Chem. 261*, 10695−10700.
(15) Ye, S. X., Huber, T., Vogel, R., and Sakmar, T. P. (2009) FTIR analysis of GPCR activation using azido probes. *Nat. Chem. Biol. 5*, 397−399.
(16) Ye, S. X., Zaitseva, E., Caltabiano, G., Schertler, G. F. X., Sakmar, T. P., Deupi, X., and Vogel, R. (2010) Tracking G-protein-coupled receptor activation using genetically encoded infrared probes. *Nature 464*, 1386−1389.
(17) Dorman, G., and Prestwich, G. D. (1994) Benzophenone photophores in biochemistry. *Biochemistry 33*, 5661−5673.
(18) Gritsan, N. P., Gudmundsdottir, A. D., Tigelaar, D., Zhu, Z., Karney, W. L., Hadad, C. M., and Platz, M. S. (2001) A laser flash photolysis and quantum chemical study of the fluorinated derivatives of singlet phenylnitrene. *J. Am. Chem. Soc. 123*, 1951−1962.
(19) Napier, C., Sale, H., Mosley, M., Rickett, G., Dorr, P., Mansfield, R., and Holbrook, M. (2005) Molecular cloning and radioligand binding characterization of the chemokine receptor CCR5 from rhesus macaque and human. *Biochem. Pharmacol. 71*, 163−172.
(20) Garcia-Perez, J., Rueda, P., Alcami, J., Rognan, D., Arenzana-Seisdedos, F., Lagane, B., and Kellenberger, E. (2011) Allosteric model of maraviroc binding to CC chemokine receptor 5 (CCR5). *J. Biol. Chem. 286*, 33409−33421.
(21) Liu, Y., Zhou, E., Yu, K., Zhu, J., Zhang, Y., Xie, X., Li, J., and Jiang, H. (2008) Discovery of a novel CCR5 antagonist lead compound through fragment assembly. *Molecules 13*, 2426−2441.
(22) Dragic, T., Trkola, A., Thompson, D. A., Cormier, E. G., Kajumo, F. A., Maxwell, E., Lin, S. W., Ying, W., Smith, S. O., Sakmar, T. P., and Moore, J. P. (2000) A binding pocket for a small molecule inhibitor of HIV-1 entry within the transmembrane helices of CCR5. *Proc. Natl. Acad. Sci. U.S.A. 97*, 5639−5644.
(23) Seibert, C., Ying, W., Gavrilov, S., Tsamis, F., Kuhmann, S. E., Palani, A., Tagat, J. R., Clader, J. W., McCombie, S. W., Baroudy, B. M., Smith, S. O., Dragic, T., Moore, J. P., and Sakmar, T. P. (2006) Interaction of small molecule inhibitors of HIV-1 entry with CCR5. *Virology 349*, 41−54.
(24) Abrol, R., Kim, S. K., Bray, J. K., Griffith, A. R., and Goddard, W. A., 3rd (2011) Characterizing and predicting the functional and conformational diversity of seven-transmembrane proteins. *Methods 55*, 405−415.
(25) Knepp, A. M., Grunbeck, A., Banerjee, S., Sakmar, T. P., and Huber, T. (2011) Direct measurement of thermal stability of expressed CCR5 and stabilization by small molecule ligands. *Biochemistry 50*, 502−511.
(26) Marti-Renom, M. A., Stuart, A. C., Fiser, A., Sanchez, R., Melo, F., and Sali, A. (2000) Comparative protein structure modeling of genes and genomes. *Annu. Rev. Biophys. Biomol. Struct 29*, 291−325.
(27) Humphrey, W., Dalke, A., and Schulten, K. (1996) VMD: Visual molecular dynamics. *J. Mol. Graph. 14*, 33−38.